

# Seven Cases Unstructured Triangulation Technique for Simplified Version of Conceptual Model of Ethylene Furnace for Radiative Heat Transfer Approximation

Abd. Samad Hasan Basari,  
Zuraida Abal Abas

Centre for Advanced Computing Technology,  
Faculty of Information & Communication  
Technology, UTeM

Shaharuddin Salleh

Department of Mathematics, Faculty of Science  
UTM

## ABSTRACT

In this paper, we introduce a new enhanced method utilizing the approach of advancing front technique for generating unstructured meshes in the simplified version of ethylene conceptual model. The method is called as Seven Cases Unstructured Triangulation Technique (7CUTT) where it is based on seven categories of cases for element creation procedure and the layer concept for mesh gradation control. The algorithm of the mesh incorporates sensor deployment in its conceptual model to supply input for boundary values. The quality of the mesh is determined based on a measurement in GAMBIT software. 7CUTT provides the framework for the heat to be approximated using the discrete ordinate method, which is a variant of the finite volume method. Simulation results produced using FLUENT support the findings for effectively approximating the flue gas temperature distribution in the simplified furnace at the end of the study.

## General Terms

Seven Cases Unstructured Triangulation Technique (7CUTT), finite volume method, discrete ordinate method.

## Keywords

Advancing front technique; element creation procedure; sensors; radiative heat transfer; discrete ordinate method

## 1. INTRODUCTION

Ethylene is an important chemical compound produced in the petrochemical industry which is produced from the steam cracking process in ethylene cracker furnaces [1]. In steam cracking, heat is used for breaking or cracking down the saturated hydrocarbon or feedstocks into smaller hydrocarbon in the coils or reactor tubes, which eventually produces desired products such as ethylene.

Radiation is a heat transfer mode which plays a significant role in ethylene production. It has been noted in [2] that 90% of the heat transfers in the furnace involve radiation. Radiation is caused by energy emission in the form of electromagnetic waves or streams of photons [3]. The burners which are located on the floor near the furnace wall heat up the furnace. This happens because the combustion process carried out in the burner results in flames and the release of its hot flue gas. The radiative heat from the furnace wall and hot

flue gas is transferred to reactor tubes/coils.

Structured or unstructured triangular mesh formation is an important step for approximating solutions to boundary value problems. One such method is the advancing front technique where the key algorithmic step is the appropriate introduction of the new elements to the empty region [4]. The method places a new element by considering an ideal point generated as well as the existing nodes in the circle constructed. The centre of the circle is the ideal point and the radius is calculated based on the empirical rules for element creation procedures. The advancing front technique is guaranteed to preserve boundary integrity as well having the capacity to create triangular elements with high aspect ratios in boundary-layer regions [5].

Another work that promotes the advancing front techniques but has a different approach from the conventional one is generating the umbrella of the triangles centred at a point of a closed curve [6]. The ordered samples of points are constructed at the curve by using an implicit equation and following some of its rules. The new edges are formed by connecting the resulting selected points at the curve to the centre of the curve. This procedure is repeated until the entire domain is triangulated. A circle packing algorithm which also utilizes the frontal method generates the unstructured mesh by connecting the centres of packing circles with specified sizes [7]. The procedure starts from any convenient point within an open domain and does not need to start from the boundary as proposed by the conventional frontal method.

In [8], the author highlighted three cases as being possible during the element creation procedure:

- (1) A new element is created with a new node as a vertex in which the new node is joined to the edge being considered.
- (2) An already existing Front node satisfying certain conditions in the proximity of the edge being considered is used to create a new element.
- (3) Neither of the cases above in which an efficient algorithm of mesh generation should be able to tackle such a problem.

In the present paper, a new algorithm called the Seven Cases Unstructured Triangulation Technique (7CUTT) is introduced, for producing initial unstructured grids based on seven categories of cases. These seven categories of cases are extensions of the normal cases as in [5, 8] and are able to solve the problems highlighted in [8], specifically the third point above. The technique takes into account the deployment

of sensor nodes as boundary nodes which supply input values into the system. The technique makes use of the layer concept. Radiative heat transfer in the simplified version of ethylene cracker furnace can be modelled using the Discrete Ordinate Method by transforming the radiative heat equations into a set of simultaneous partial differential equations based on a discrete representation of the directional variation of the radiative intensity [3].

## 2. PROBLEM STATEMENT

The problem can be stated as follows: Given a set of sensors distributed along the wall of the simplified version of ethylene furnace, in what way can the sensors be deployed to provide input in the form of boundary values to approximate the flue gas temperature inside the furnace?

In this problem, the approximation based on the two-dimensional cross-section of the furnace involving cases with an arbitrary number of sensors is discussed. As an initial study for the conceptual model, a simplified case is studied as shown in Figure 1 by assuming that half of the coil (a single circle) is placed at the centre of the furnace.

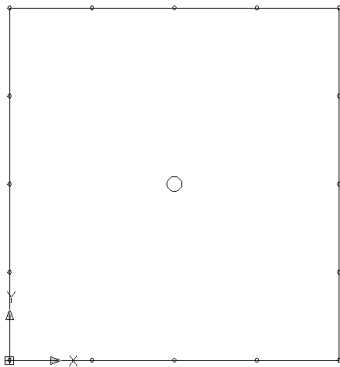


**Fig 1 A simplified problem domain for the initial study with only 1 circle representing half a reactor coil**

This paper focuses on improving the initial unstructured grids by enhancing the existing standard method in order to have a mesh which satisfies the requirement of having the sensors placed at the boundary as the nodes for the boundary elements as well as incorporating this with a way to control the size and shape of the triangular mesh generated. Besides that, the method needs to be able to construct the triangular element directly in every iteration, so that no re-order of the front or deletion of the existing element is required to perform triangulation. It is assumed that the sensors (represented by 16 smaller circles) are placed in the conceptual model as illustrated in Figure 1.

## 3. THE GENERAL BASIC STEP OF THE STANDARD ADVANCING FRONT TECHNIQUE (SAFT)

The boundary curves are discretized by dividing them into straight line segments or edges where nodes are placed on each of the segments or edges. An edge is denoted as  $(a, b)$  which means that the edge is formed by nodes  $a$  and  $b$ . Figure 2a illustrates a simple two dimensional domain with connected boundary curves while Figure 2b illustrates the discretized boundary curves into a set of edges denoted by  $(1, 2), (2, 3)$  until  $(10, 1)$ .

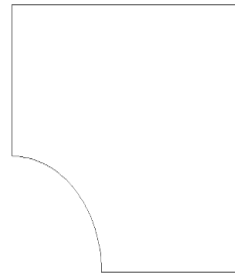


**Fig 2a A two dimensional domain with connected boundary curves**

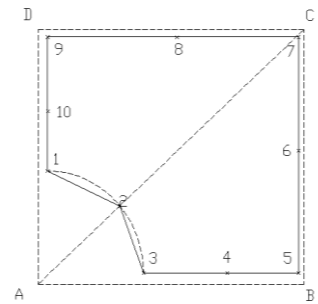


**Fig 2b A set of edges forming initial Front and the background grid consisting of triangles ABC and ADC**

Front [5, 8] is a list or a set of active edges which is currently available for element triangulation. Referring to Figure 2b, all the edges which are  $(1, 2), (2, 3), (3, 4)$  until  $(10, 1)$  from the first or initial Front. The Front is updated continuously when a triangular element is created. This can be seen in Figure 3, taken from [9]. It must be noted that all the edges belonging to the current Front are considered as active edges while edges that are deleted from the current Front list are considered as passive edges. Any nodes which compose the active edges in the current position of the Front list are also known as active nodes.

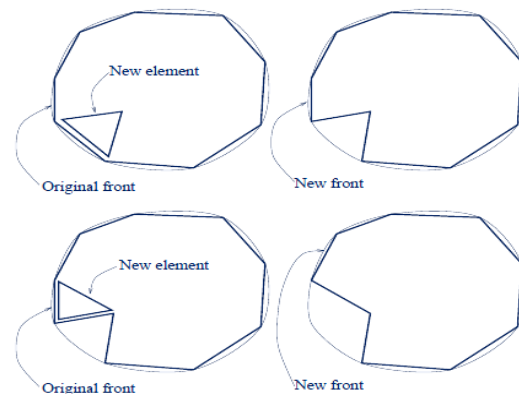


**Fig 3 The illustration of elements with regards to Front, taken from [9]**

The main approach to controlling the grid in terms of the size and shape of the triangular element involves the definition of the required grid-cell characteristic through background grid generation [4, 5, 8, 10-13]. The grid-cell characteristics, known as grid cell parameters, are the size

parameter  $\delta$ , the stretching  $s$  and finally the orientation of the cells  $\phi$  [5]. For example, Figure 2b illustrates the background grid consisting of two triangles ABC and ADC. The grid cell parameters are required to be specified at each node forming the background grid where in this example at nodes A, B, C and D. In the creation of the triangular element, once the edge is selected from the Front for triangulation, the position of ‘ideal’ point (IP)[5] on the perpendicular bisector of the edge is computed in such a way that an equilateral triangle is formed with IP as the third vertex. Figure 4a illustrates a selected edge, which is (a, b) and the position of the IP.

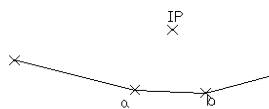


**Fig 4a The selected edge (a,b) and the position of IP**

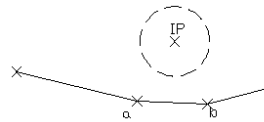


**Fig 4b A circle is constructed with its centre at IP and the radius of the circle following the empirical rule.**

Grid cell parameters for all nodes in the Front are interpolated [5]. The edge with the shortest length  $l$  in the Front is selected as a departure zone in order to create the triangular element. In order to obtain  $\delta$  for the next step of calculation, the interpolated values of  $\delta$  corresponding to the two nodes of the edge are averaging. A circle with centre at IP is constructed with the following empirical formula for the radius,  $r = 0.8 * \delta'$ , where [5]

$$\delta' = \begin{cases} 0.55 * l; & \delta < 0.55 * l \\ \delta; & 0.55 * l \leq \delta \leq 2.0 * l \\ 2.0 * l; & \delta > 2.0 * l \end{cases} \quad (1)$$

Figure 4b illustrates a circle with its centre at IP and the radius of the circle following the empirical rule. Active nodes that lie within the circle are searched (if any) and their distances from IP are listed. The best candidate for the third vertex of the triangular element would be the closest one to the IP. The equilateral triangle is constructed if there are no such active nodes lying within the circle. However, the validity of the IP becoming the node must be checked, by which it needs to satisfy the following conditions [5]:

- (1) The coordinate of IP does not lie inside another existing triangular element,
- (2) There is no intersection between the side of the new triangular element and any existing sides of the active front.

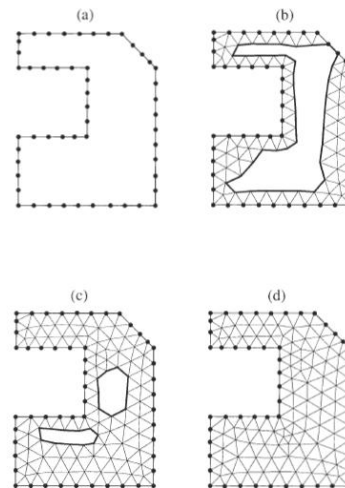


**Fig 5 The illustration of the Front ‘marching’ process into the interior of the domain, taken from [14]**

Generally, the Front progresses into the interior of the domain in a ‘marching’ [5, 14] process as a result of producing a triangular element in which new nodes and edges are created and at the same time old related edges are deleted, as illustrated in Figure 5. The new triangular element is constructed by two nodes of a segment of a Front and another node, either a newly created one or one that has already existed in the Front. This process is continued until there are no longer any active edges in the Front list.

#### **4. THE SEVEN CASES UNSTRUCTURED TRIANGULATION TECHNIQUE (7CUTT) ALGORITHM**

The contribution of this paper is a new algorithm called the *Seven Cases Unstructured Triangulation Technique* for the initial triangular mesh generation (7CUTT). 7CUTT is a newly developed algorithm for initial unstructured triangulation grid generation with a slight modification to the SAFT in terms of element creation and the control grid. The algorithm of 7CUTT is applicable to the domain with single or multiple inner boundaries. It still uses the concept of the SAFT where the Front is moved into the interior of the domain in a ‘marching’ process when constructing triangular elements. It must be noted that the terms ‘edge’, ‘Front’, ‘active edge’, ‘passive edge’, ‘active node’ and ‘ideal point’ (IP) in 7CUTT are similar to those explained in SAFT in section 3.

The endpoints of outer boundary curves in the domain are the first set of nodes created in order to prepare for the triangular mesh generation. This is followed by all the nodes created at the boundary curves resulting from discretising boundary curves (both inner and outer boundaries) into boundary edges. As illustrated in Figure 6a, the boundary curves are discretised into a number of outer boundary edges (from the outer layer boundary) and a number of internal boundary edges (from the internal boundary layer). It must be noted that in the 7CUTT algorithm, nodes are placed at the location of sensor deployment where a boundary edge is formed automatically between two sensors.

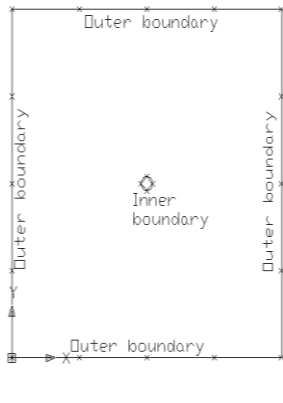


Fig 6(a) Definition of boundary edges at boundary curves

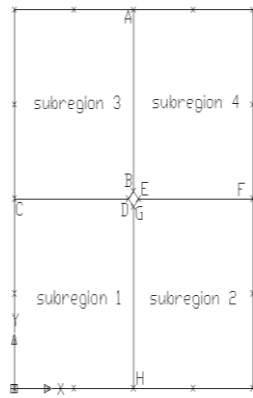


Fig 6(b) The whole domain is divided into sub-regions

### 4.1 The Layer Concept

It must be noted that the layer concept is a novel contribution of this study. 7CUTT makes use of the layer concept at the appropriate boundary curve or line. The aim of employing the layer concept is to divide a line into several segments with different lengths linearly. The length  $Ld_i$  of layer  $d_i$  with  $i = 1, 2, \dots, m$  is given as

$$Ld_i = i \frac{L}{\sum_{k=1}^m k} \quad (2)$$

In the above equation,  $L$  is the total length of the straight line while  $m$  is the number of layers needed.

The line or boundary curve that is divided using the layer concept produces several smaller line segments with different length linearly. A set of nodes is placed at the end of each newly divided segment line. Figure 7a illustrates a straight line before having the layer concept while Figure 7b illustrates  $m$  number of smaller segment lines or edges resulted from the layer concept applied at AB. For illustration, let say the length of the straight line AB as in Figure 7a is  $L = 1.34$  and the number of layers required is  $m = 6$ . Table 1 shows the layer and its length for every layer of Figure 7b.



Fig 7(a) A straight line AB before applying layer concept

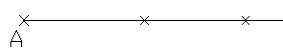


Fig 7(b) A set of nodes are placed at the line segments produced by employing layer concept at line AB

Table 1 The result for the layer concept for Figure 4.3b

Layer $d_i$	Length of layer, $Ld_i$
$d_1$	$Ld_1 = (1) \frac{1.34}{1+2+3+4+5+6} = 0.0638$
$d_2$	$Ld_2 = (2) \frac{1.34}{1+2+3+4+5+6} = 0.1276$
$d_3$	$Ld_3 = (3) \frac{1.34}{1+2+3+4+5+6} = 0.1914$
$d_4$	$Ld_4 = (4) \frac{1.34}{1+2+3+4+5+6} = 0.2552$
$d_5$	$Ld_5 = (5) \frac{1.34}{1+2+3+4+5+6} = 0.3190$
$d_6$	$Ld_6 = (6) \frac{1.34}{1+2+3+4+5+6} = 0.3830$

In the present study, the layer concept is proposed to be applied once the whole domain is divided into sub-regions, where it is employed to generate the segment lines at the appropriate boundary of the sub-region. This can be referred to in Figure 8 where the layer concept is applied at newly created line segments AB, CD, EF and GH. The gap of length between all the edges is reduced with the existence of these sets of newly created line segments. Therefore, the layer concept is served as an interior gradation control as it is incorporated in the algorithm of 7CUTT. However, it must be noted that the entire front needs to be chosen (starting from edge with the shortest length condition) for the departure zone or the element creation zone in order to have a full effect of gradation control in terms of size using the layer concept.

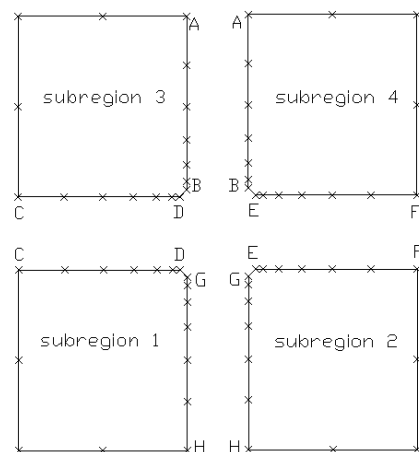
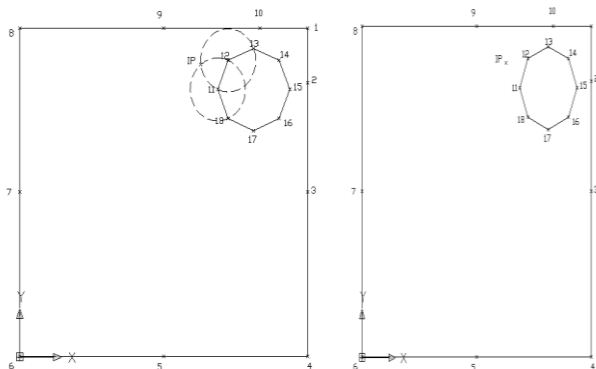


Fig 8 Applying the layer concept at the newly created line segment (the newly created boundary of the sub-regions- AB, CD, EF and GH)

## 4.2 The General Idea of the 7CUTT and the Algorithm

In 7CUTT, the current selected active edge among all the active edges in the Front that is considered for triangular element construction is called the base edge. For example, referring to Figure 9a, of all the active edges in the Front, (11, 12) are currently selected for triangular element construction therefore; (11, 12) is called a base edge. Once the base edge is identified, the position of IP on the perpendicular bisector of the base edge is computed in such a way that an equilateral triangle is formed with IP as the third vertex. Let us say the length of the base edge is denoted as  $L_{base\_edge}$ .

The easiest way to compute the IP satisfying the above condition is to form a circle (with a radius equal to  $L_{base\_edge}$  and centred at the nodes respectively) at each node of the base edge as illustrated in Figure 10a. Basically, there are two intersection points at first, but the one that lies inside the Front or inside the acceptance region is chosen. The chosen intersection point of these two circles is the IP. The two circles constructed previously are deleted in order to avoid confusion while the IP remains in the domain as illustrated in Figure 9b.



**Fig 9(a) The base edge is (11,12). Intersection point of the two circles is the IP**

**Fig 9(b) IP on the perpendicular bisector of the base edge**

A circle with its centre at IP is constructed with a radius,  $r = 0.8 * L_{base\_edge}$  as illustrated in Figure 9c. IP becomes the new vertex of the equilateral triangle constructed since there are no active nodes lying within the circle and two newly created active edges are formed automatically as illustrated in Figure 9d. It must be noted that once the triangular element is constructed, the Front needs to be updated in which the base edge becomes a passive edge and is deleted from the Front list. At the same time, the newly created active edges are added to the Front list. Having Figure 10d as an example, (11, 12) is deleted and newly created edges which are (11, 19) and (19, 12) are added to the Front list.

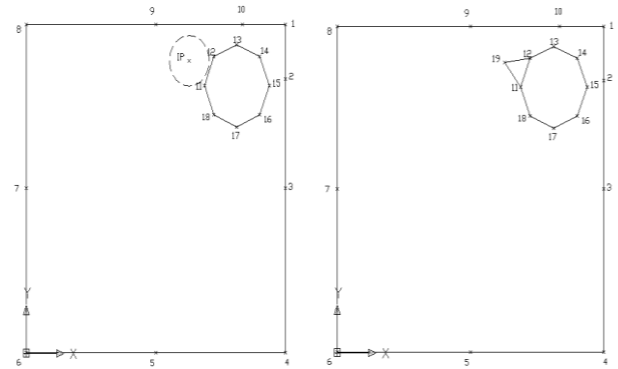


**Fig 9(c) A circle is constructed with IP as centre**

**Fig 9(d) A triangular element is constructed by having IP as the node**

The same procedure is repeated to construct the next triangular element, in which base edge is selected, IP is constructed and a circle with radius equal to eighty percent of the length of the base edge and its centre at IP is constructed. A construction of triangular elements using the algorithm of 7CUTT is actually based on the condition of objects lying within the circle or at the circum circle. The term ‘objects’ in 7CUTT refers to any active nodes or active edges. This is where the construction of the initial unstructured triangular element is based on seven cases of consideration during the element creation procedure according to the 7CUTT algorithm.

## 4.3 The algorithm of 7CUTT

The 7CUTT with specific Front as departure zone starting with the shortest edge is summarized as follows:

**Step 1:** Generate nodes at the outer boundary based on the pre-determined location on the sensors. Generate inner boundary nodes. The whole computational domain is then divided into M number of sub-regions. Apply the layer concept at the desired location along the boundary of the sub-region.

**Step 2:** From the nodes at the boundary, boundary edges will be formed. The set of all boundary edges (at outer, inner boundary as well as at sub-region boundary) will now be the Initial Front. Start to generate triangular elements at sub-region 1.

**Step 3:** The inner boundary edge will be chosen first to be triangulated. The current selected edge being considered is called the base edge.

**Step 4:** Compute the ideal point (IP) on the perpendicular bisector of the base edge in such a way that an equilateral triangle is formed with the IP as vertex.

**Step 5:** Construct a circle with a radius  $r = 0.8 * L_{base\_edge}$ . Determine if any objects such as active nodes lie within the circle or intersected active edges with the circum circle.

**Step 6:** Generate the triangular elements based on the seven categories of cases below:

**Case 1:** No active nodes or active edges lie within the circle. The IP is selected as the vertex. Equilateral triangle will be formed.

**Case 2:** Active nodes lie within the circle. Compute the distance of all the active nodes and the IP. The closer point to the IP will be selected as the vertex.

**Case 3:** Three active edges are connected to themselves. Therefore, the three edges will automatically form a triangular element.

**Case 4:** No active node lies within the circle. However, there is an active edge intersecting with the circle but  $L_{p1p2} < r$ . Therefore, the intersected active edge is disregarded and instead the IP will become the vertex.

**Case 5:** No active node lies within the circle. However, there is active edge intersecting with the circle. At the same time, both  $L_{p1p2} \geq r$  and  $L_{ie} < 2 * L_{base\_edge}$  are satisfied. Therefore, the nodes associated with the intersected edge will be considered in which the node that is closer to the IP will be selected as the vertex to form a new element.

**Case 6:** No active node lies within the circle. However, there is an active edge intersecting with the circle. At the same time, three conditions  $L_{p1p2} \geq r$ ,

$$L_{ie} \geq 2 * L_{base\_edge} \quad \text{and} \quad \frac{L_p}{L_{ie}} < 0.1 \text{ are satisfied.}$$

Therefore, the active edge intersecting with the circle is considered in which the node of the intersected active edge is selected as the third vertex.

**Case 7:** No active node lies within the circle. However, there is an active edge intersecting with the circle. At the same time, three conditions  $L_{p1p2} \geq r$ ,

$$L_{ie} \geq 2 * L_{base\_edge} \quad \text{and} \quad \frac{L_p}{L_{ie}} \geq 0.1 \text{ are satisfied.}$$

Therefore, two new elements will be constructed.

**Step 7:** Update the Front by deleting the base edge. The new active edges created during the triangulation element will be added in the Front list.

**Step 8:** If there are still inner boundary edges left, repeat Steps (4) to (7) until all inner boundary edges have been triangulated from the Initial Front list. If there is only one inner boundary edge, go directly to Step (9).

**Step 9:** Select the active edge with the shortest length in departure zone group. The current selected edge being considered is called the base edge. Repeat Step (4) - Step (7) until all the active edges in the departure zone group in the current Front become passive.

**Step 10:** Construct a new Front list composed of all the newly created edges together with the available active edges from the previous Front.

**Step 11:** Select the active edge with the shortest length in the departure zone group of the latest updated Front list. The current selected edge being considered is called the base edge. Repeat Step (4)-Step (7) until all the edges of the departure zone become passive edges.

**Step 12:** Step (10) - Step (11) are repeated until there is no more active edge to compose the Front, which means the entire sub-region 1 has been completely triangulated.

**Step 13:** Repeat Step (3) - Step (12) for the next sub-region until all M number of sub-regions have been triangulated, which means that the whole computational domain has been completely triangulated.

## 5. SIMULATIONS AND RESULTS

Simulation is performed using FLUENT version 6.0 on an arbitrary number of sensors placed at various points along the inner wall of the furnace as can be seen in Figure 1. A set of nodes are placed at the pre-determined locations of the sensors where a set of outer boundary edges are generated. Four pivot points are placed at the inner boundary representing the reactor coil where a set of inner boundary edges are generated. The layer concept is incorporated as illustrated in Figure 8. The result of unstructured mesh with 7CUTT incorporating the layer concept is illustrated in Figure 10.

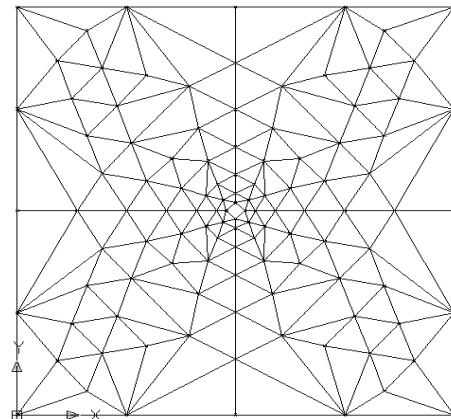


**Fig 10 The resulting initial unstructured mesh using the algorithm of 7CUTT for the simplified conceptual model as in Figure 1.**

The sizes of the triangular elements gradually increase from the centre of the furnace where the reactor coils are located towards the furnace wall. This is because the set of edges of varying length linearly which results from the layer concept applied at the boundary of the sub-domain, can tolerate the difference between the shortest length of edges (at the inner boundary) and the longest length of edges (at the outer boundary). Therefore, the element size is increasing gradually with the existence of edges from the layer concept, since the creation of the triangular element in 7CUTT is based on the inner boundary edges and edges from the layer concept at the boundary of sub-regions as the departure zone starting with the shortest active edges.

In order to examine the quality of the mesh, an EquiAngle Skew  $Q_{EAS}$ , which is a normalized measure of skewness that is defined as follows is used [15]

$$Q_{EAS} = \max \left\{ \frac{\theta_{max} - \theta_{eq}}{180 - \theta_{eq}}, \frac{\theta_{eq} - \theta_{min}}{\theta_{eq}} \right\} \quad (3)$$

In the above equation,  $\theta_{max}$  and  $\theta_{min}$  are the maximum and minimum angles (in degrees) between the edges of the triangular element and  $\theta_{eq}$  is the characteristic angle corresponding to an equilateral element of a triangular element where in this particular case,  $\theta_{eq} = 60^\circ$ . The value of the examined quality based on this equation provided by [15] is in the range of  $0 \leq Q_{EAS} \leq 1$  where  $Q_{EAS} = 0$  if the element is an equilateral triangle and  $Q_{EAS} = 1$  if the triangular element is degenerate (poorly shaped). Figures 11(a) – Figure 11(d) illustrate the corresponding triangular elements in the mesh with respect to the range of the quality examined.

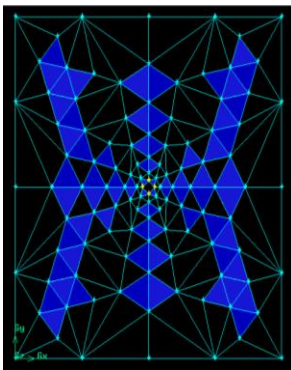


**Fig 11(a) Element with quality  $Q_{EAS} = 0$**

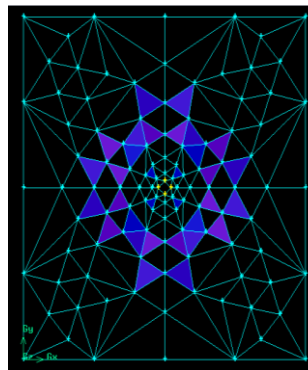


**Fig 11(b) Element with quality  $0 < Q_{EAS} \leq 0.25$**

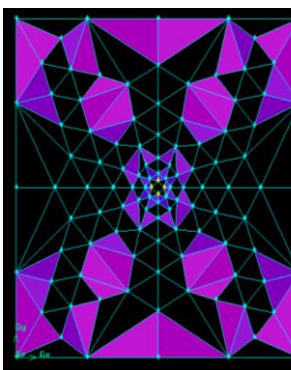


**Fig 11(c) Element with quality  $0.25 < Q_{EAS} \leq 0.5$**

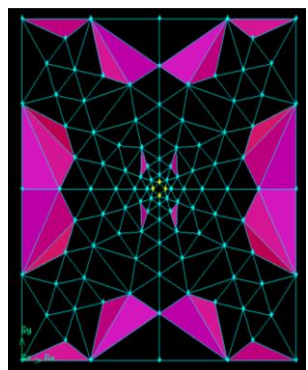


**Fig 11(d) Element with quality  $0.5 < Q_{EAS} \leq 0.75$**

Of all the triangular elements generated, 35.29% are equilateral triangles and 13.73% fall into the average or fair quality range  $0.5 < Q_{EAS} \leq 0.75$  where the highest value

for the element quality is  $Q_{EAS} = 0.7119$ . The overall relationship between  $Q_{EAS}$  and element quality is illustrated in Table 2 [15]. The total number of elements in percentages with respect to the range of element quality can be referred to the same table. It can be seen that the initial triangular elements generated using the 7CUTT are all valid and independent of its size as well as none of them being degenerate or poorly shaped.

**Table 2 The relationship between  $Q_{EAS}$  and mesh quality together with the total elements in the range respectively for unstructured grids generated with CBATT for the domain of one circle as in Figure 19.**

$Q_{EAS}$	Mesh quality	Total element in percentage
$Q_{EAS} = 0$	Equilateral	35.29%
$0 < Q_{EAS} \leq 0.25$	Excellent	15.69%
$0.25 < Q_{EAS} \leq 0.5$	Good	35.29%
$0.5 < Q_{EAS} \leq 0.75$	Fair	13.73%
$0.75 < Q_{EAS} \leq 0.9$	Poor	0%
$0.9 < Q_{EAS} \leq 1$	Very poor	0%
$Q_{EAS} = 1$	Degenerate	0%

In order to prove that the resulting unstructured triangular mesh using the algorithm of 7CUTT works well and is appropriate for computational analysis, the governing equation of radiative heat transfer is incorporated with the mesh for the simplified conceptual model. Using FLUENT version 6.0, simulation is conducted to solve the radiative heat transfer by using the Discrete Ordinate Method. Since this is a conceptual model, the value of the wall temperature at every sensor is imposed so that the temperature value can be used as boundary values in the calculation. The simulation is conducted until convergence is reached for both models. The plot of convergence for the model can be referred to Figure 12 while the simulation result of the contour plot of temperature (K) distribution for the flue gases in the furnace can be seen in Figure 13.

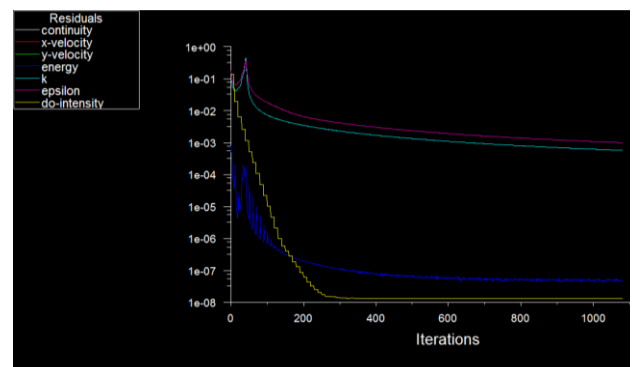


**Fig 12 The plot of convergence for simplified conceptual model with one circle**

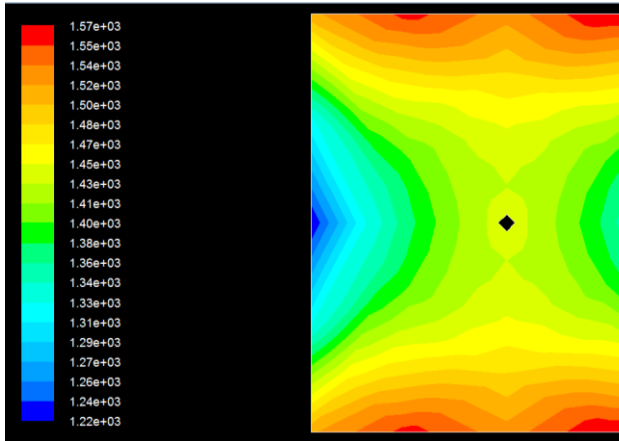


**Fig 13 The contour of temperature (K) distribution of the flue gas for the domain of simplified conceptual model.**

## 6. SUMMARY AND CONCLUSION

A new technique called 7CUTT is proposed which is proven to be effective in generating initial unstructured grids/meshes for modelling the simplified version of conceptual model of integrating sensors and radiative heat transfer in ethylene cracker furnaces. 7CUTT incorporates the layer concept to generate nodes which form edges of varying lengths linearly at appropriate boundary curves as well as introducing the structured seven cases for the element creation procedure. The triangular mesh forms the domain for approximating the radiative heat transfer using the Discrete Ordinate Method. Simulations using FLUENT are performed on the triangular mesh to obtain the numerical approximations. The results obtained support the findings in 7CUTT for effectively generating the unstructured mesh in the process of approximating the temperature of flue gas in the furnace. It must be noted that the novel contribution of the paper is in the method of producing initial unstructured grids and the interior gradation control but not the numerical method of the Discrete Ordinate Methods.

## 7. ACKNOWLEDGMENTS

The authors would like to thank the Malaysian Ministry of Higher Education and Universiti Teknikal Malaysia Melaka for their financial funding through SLAI for PhD scholarship.

## 8. REFERENCES

[1] Gielen, D., K. Bennaceur, and C. Tam. IEA Petrochemical Scenarios for 2030-2050: Energy Technology Perspectives. 2006 [cited 2008 17 Dec]; Available from: [http://www.iea.org/textbase/work/2006/petrochemicals/Discussion\\_Paper.pdf](http://www.iea.org/textbase/work/2006/petrochemicals/Discussion_Paper.pdf).

[3] Heynderickx, G.J. and M. Nozawa, High-emissivity coatings on reactor tubes and furnace walls in steam cracking furnaces. *Chemical engineering science*, 2004: p. 5567-5662.

[4] Modest, M.F., *Radiative Heat Transfer*. 2 ed. 2003: Academic Press. 822.

[5] Lohner, R., *Progress in Grid Generation via the Advancing Front Technique*. *Engineering with Computers*, 1996: p. 186-210.

[6] Farrashkhalvat, M. and J.P. Miles, *Basic structured grid generation with an introduction to unstructured grid generation*. 2003: Butterworth Heinemann.

[7] Hernández-Mederos, V., P.L.d. Ángel, and J. Estrada-Sarlabous, Isotropic umbrella based triangulation of regular parametric surfaces. *Numer Algor*, 2008. **48**: p. 29–47.

[8] Wang, W.X., C.Y. Ming, and S.H. Lo, Generation of triangular mesh with specified size by circle packing. *Advances in Engineering Software*, 2007. **38**: p. 133-142.

[9] Kovac, N., S. Gotovac, and D. Poljak, A New Front Updating Solution Applied to Some Engineering Problems. *Archives of Computational Methods in Engineering*, 2002. **9**: p. 43-75.

[10] Persson, P.-O., *Lecture 1 Computational Mesh Generation*. 2008, MIT.

[11] Zhu, J., T. Blacker, and R. Smith, Background overlay grid size functions, in *Proceedings of the 11th international meshing roundtable*. 2002. p. 65–74.

[12] Lyra, P.R.M. and D.K. Carvalho, A computational methodology for automatic two-dimensional anisotropic mesh generation and adaptation. *Journal of the Brazilian Society of Mechanical Sciences and Engineering*, 2006. **28**(4): p. 399-412.

[13] Seveno, E. *Towards an adaptive advancing front method*. in *6th International Meshing Roundtable*. 1997.

[14] Peraire, J., J. Peiro, and K. Morgan, *Advancing front grid generation*, in *Handbook of Grid Generation*, N.P. Weatherill, B.K. Soni, and J.F. Thompson, Editors. 1999, CRC Press LLC.

[15] Blazek, J., *Principles of Grid Generation*, in *Computational Fluid Dynamics: Principle and Applications*. 2007.

[16] *Gambit 2.3 Documentation - Gambit User Guide*. [cited 2010 25 November]; Available from: <http://my.fit.edu/itresources/manuals/gambit2.3/help/index.htm>.